



An implicit gradient model by a reproducing kernel strain regularization in strain localization problems

Jiun-Shyan Chen ^{a,*}, Xinwei Zhang ^a, Ted Belytschko ^b

^a *Department of Civil and Environmental Engineering, University of California, Los Angeles, 5731 Boelter Hall, Los Angeles, CA 90095-1593, USA*

^b *Department of Mechanical Engineering, Northwestern University, 2145 N. Sheridan, Evanston, IL 60208-3111, USA*

Received 13 September 2003; received in revised form 15 December 2003; accepted 17 December 2003

Abstract

A reproducing kernel strain regularization (RKSR) as a mathematical generalization of gradient theory and non-local theory for strain localization problems is presented. RKSR introduces a correction of the weight function in the non-local strain by imposition of gradient reproducing conditions. Both continuum and discrete forms of RKSR are presented, and they lead to an implicit representation of gradient models. As such, RKSR provides a gradient type regularization to the localization problem without increasing the order of differentiation in the governing equations. Hence no additional boundary conditions are required, and the need for higher order continuity for the approximation of unknowns in the governing equations is no longer an issue. A von Neumann spectral analysis is employed to study the spectral properties of RKSR of various orders in one dimension. It is shown that RKSR almost duplicates the spectral properties of second and fourth order gradient theories. In summary, RKSR reproduces the regularization properties of gradient methods without dealing with additional boundary conditions or higher order continuity issues.

© 2004 Elsevier B.V. All rights reserved.

Keywords: Strain localization; Implicit gradient model; Gradient reproducing conditions; Strain regularization; Damage mechanics

1. Introduction

Strain localization is usually a precursor of catastrophic material failure. In geomaterials, such as soils, concrete, rocks, strain localization has been observed in a variety of situations, such as triaxial tests in the lab [18] and earth excavation processes in the field [15]. When the classical continuum theory is adopted directly to softening materials, the corresponding boundary value problem changes type and cannot describe the underlying physics correctly. This difficulty arises because solutions possess features of measure

* Corresponding author.

E-mail addresses: jschen@seas.ucla.edu (J.-S. Chen), tedbelytschko@northwestern.edu (T. Belytschko).

zero [4,6], so characteristic length of the mesh introduces a mesh-size perturbation. The dependence on the discretization is not only with respect to mesh refinement but is also with respect to the mesh alignment.

The inability of the classical continuum theory to describe the discontinuous strain fields can be corrected if the discontinuous strain field is regularized (smoothed). One viable approach is to consider microstructure such as microcrack distributions near strain localization zone so as to smooth the discontinuous strain field and thus regularize the equations. The microstructure can be homogenized to provide an additional length scale as a correction of the classical continuum theory. Many regularization techniques, such as rate-dependent models [16,24,28], Cosserat models [23], gradient method [12,13,19], and non-local theory [3] introduce internal length scales that can be related to the microstructure of softening materials. For example, the Cosserat model is obtained by generalizing the kinematic relations with additional rotational degrees to represent the local rotation of microstructure. Generalization of the constitutive equations by including higher order spatial derivatives in gradient and non-local methods also introduce additional length scales. Some studies have been made to justify the characteristic length in the non-local theory from microstructure [5].

In non-local theory, the stress at a point is related to the distribution of strain in the neighborhood via a weighted average. The domain of influence in the weight function introduces an internal length scale to the continuum measure of deformation. However, several computational issues hamper non-local theory. The weighted averaging process introduces incompatibility between local and non-local variables. For example, the unbalanced approximation of local and non-local strains can lead to stress oscillations. The averaged stress–strain relation is no longer one to one for each material point, and this complicates the formulation of an inconsistent tangent operator in the incremental equations. In addition, for plasticity and damage computation, a complicated return mapping scheme is needed.

Gradient method can be related to non-local theory by a Taylor series expansion [25]. Both second order and fourth order gradient models have been proposed [1,2,19]. However, introducing gradient terms in the governing equation increases the order of differentiation and thus requires higher order continuity in the approximation of displacement. Also, to meet equilibrium in the second order gradient model, the normal derivative of strain should vanish along the boundaries. For the same reason, both the first and third normal derivatives of strain should vanish along the boundaries in the fourth order gradient model [2]. Until now, the physical explanation of these additional boundary conditions is still lacking [14]. The above mentioned difficulties have been addressed by some recent studies. Askes et al. [2] used a moving least square approximation [7,8] to achieve an arbitrary order of continuity in the approximation field variables in strain localization problems. The issue of additional boundary conditions has been addressed by introducing an intrinsic length scale through a reproducing kernel regularization of strain so that the second order gradient model can be reproduced without explicitly increasing the order of differentiation in the governing equation [9] and thus resolving the dilemma of additional boundary conditions.

In this paper, we propose a reproducing kernel strain regularization (RKSR) as an implicit representation of gradient models. By imposing the gradient reproducing conditions on the corrected weight function for the non-local strain expression, strain gradients of arbitrary order can be reproduced. This implicit representation of the gradient type regularization avoids the drawbacks of non-physical boundary conditions and higher order continuity that plague conventional gradient models. In this paper, the continuous formulation of RKSR is first introduced to demonstrate the fundamental concept. The discrete RKSR is then introduced; the discrete form is preferable because it ensures that the gradient reproducing conditions are satisfied by the numerical algorithm.

The paper is organized as follows. Section 2 introduces the continuous form of RKSR and identifies the relationship between RKSR and different forms of gradient models. In Section 3, the discrete form of RKSR is presented. The Galerkin formulation of the governing equations regularized by RKSR based on an assumed strain method is discussed in Section 4. An example demonstrating mesh-insensitive results

obtained using the proposed RKSR in a damage induced strain localization problem is also presented in this section. In Section 5, a von Neumann spectral analysis of RKSR is given and compared with gradient models. Concluding remarks are drawn in Section 6.

2. Continuum reproducing kernel strain regularization

In this section, we first formulate reproducing kernel strain regularization (RKSR) [9] as a mathematical generalization of the non-local [3] and gradient theories [12,13,19]. In these non-local theories [3], the local strain ε is regularized by the following:

$$\tilde{\varepsilon}(\mathbf{x}) = \int_{\Omega} w_a(\mathbf{x} - \mathbf{s})\varepsilon(\mathbf{s}) \, d\mathbf{s}, \tag{2.1}$$

where w_a is a weight function, $w_a(\mathbf{d}) > 0$ for $\|\mathbf{d}\| < a$, $w_a(\mathbf{d}) = 0$ for $\|\mathbf{d}\| \geq a$, and a is the radius of the support of the weight function. In [9], we introduced the following kernel regularization of the strain:

$$\tilde{\varepsilon}(\mathbf{x}) = \int_{\Omega} \tilde{w}_a(\mathbf{x}; \mathbf{x} - \mathbf{s})\varepsilon(\mathbf{s}) \, d\mathbf{s}, \tag{2.2}$$

where $\tilde{w}_a(\mathbf{x}; \mathbf{x} - \mathbf{s})$ is a regularized weight function expressed as

$$\tilde{w}_a(\mathbf{x}; \mathbf{x} - \mathbf{s}) = \left(\sum_{i+j=0}^n (x_1 - s_1)^i (x_2 - s_2)^j b_{ij}(\mathbf{x}) \right) w_a(\mathbf{x} - \mathbf{s}) \equiv \mathbf{H}^T(\mathbf{x} - \mathbf{s})\mathbf{b}(\mathbf{x})w_a(\mathbf{x} - \mathbf{s}), \tag{2.3}$$

where $\mathbf{H}^T(\mathbf{x} - \mathbf{s}) = [1, x_1 - s_1, x_2 - s_2, \dots, (x_1 - s_1)^n, (x_2 - s_2)^n]$ is an n th order monomial basis, and $\mathbf{b}(\mathbf{x})$ is the coefficient vector obtained by imposing the gradient reproducing conditions as follows. First, consider a gradient model of the following general form:

$$\tilde{\varepsilon}(\mathbf{x}) = \varepsilon(\mathbf{x}) + \sum_{i+j=1}^n \alpha_{ij} D_{ij} \varepsilon(\mathbf{x}), \tag{2.4}$$

where $D_{ij}(\cdot) = \partial^{i+j}(\cdot) / \partial x_1^i \partial x_2^j$ is a differential operator. To relate (2.2) to the gradient theory of Eq. (2.4), the following n th order gradient reproducing conditions are imposed on the regularized weight function \tilde{w}_a :

$$\int_{\Omega} s_1^p s_2^q \tilde{w}_a(\mathbf{x}; \mathbf{x} - \mathbf{s}) \, d\mathbf{s} = x_1^p x_2^q + \sum_{i+j=0}^n \alpha_{ij} D_{ij}(x_1^p x_2^q), \quad 0 \leq p + q \leq n, \quad \alpha_{00} = 0. \tag{2.5}$$

The above equation can be recast as:

$$\int_{\Omega} (x_1 - s_1)^p (x_2 - s_2)^q \tilde{w}_a(\mathbf{x}; \mathbf{x} - \mathbf{s}) \, d\mathbf{s} = \delta_{p0} \delta_{q0} + \alpha_{pq} (-1)^{p+q} p!q!, \quad 0 \leq p + q \leq n, \quad \alpha_{00} = 0. \tag{2.6}$$

By introducing Eq. (2.3) into Eq. (2.6), we have

$$\left(\int_{\Omega} (x_1 - s_1)^p (x_2 - s_2)^q \mathbf{H}^T(\mathbf{x} - \mathbf{s}) w_a(\mathbf{x} - \mathbf{s}) \, d\mathbf{s} \right) \mathbf{b}(\mathbf{x}) = g_{pq},$$

$$g_{pq} = \delta_{p0} \delta_{q0} + \alpha_{pq} (-1)^{p+q} p!q!, \quad 0 \leq p + q \leq n, \quad \alpha_{00} = 0. \tag{2.7}$$

The explicit expression of Eq. (2.7) for $0 \leq p + q \leq n$ is

$$\begin{aligned}
 \left(\int_{\Omega} \mathbf{H}^T(\mathbf{x} - \mathbf{s}) w_a(\mathbf{x} - \mathbf{s}) \, d\mathbf{s} \right) \mathbf{b}(\mathbf{x}) &= 1 = g_{00}, \\
 \left(\int_{\Omega} (x_1 - s_1) \mathbf{H}^T(\mathbf{x} - \mathbf{s}) w_a(\mathbf{x} - \mathbf{s}) \, d\mathbf{s} \right) \mathbf{b}(\mathbf{x}) &= -\alpha_{10} = g_{10}, \\
 \left(\int_{\Omega} (x_2 - s_2) \mathbf{H}^T(\mathbf{x} - \mathbf{s}) w_a(\mathbf{x} - \mathbf{s}) \, d\mathbf{s} \right) \mathbf{b}(\mathbf{x}) &= -\alpha_{01} = g_{01}, \\
 \left(\int_{\Omega} (x_1 - s_1)^2 \mathbf{H}^T(\mathbf{x} - \mathbf{s}) w_a(\mathbf{x} - \mathbf{s}) \, d\mathbf{s} \right) \mathbf{b}(\mathbf{x}) &= 2\alpha_{20} = g_{20}, \\
 &\vdots \\
 \left(\int_{\Omega} (x_2 - s_2)^n \mathbf{H}^T(\mathbf{x} - \mathbf{s}) w_a(\mathbf{x} - \mathbf{s}) \, d\mathbf{s} \right) \mathbf{b}(\mathbf{x}) &= \alpha_{0n} (-1)^n n! = g_{0n}.
 \end{aligned} \tag{2.8}$$

The above equations can be expressed in the following form

$$\mathbf{M}(\mathbf{x}) \mathbf{b}(\mathbf{x}) = \mathbf{g}, \tag{2.9}$$

where

$$\mathbf{M}(\mathbf{x}) = \int_{\Omega} \mathbf{H}(\mathbf{x} - \mathbf{s}) \mathbf{H}^T(\mathbf{x} - \mathbf{s}) w_a(\mathbf{x} - \mathbf{s}) \, d\mathbf{s}, \tag{2.10}$$

$$\mathbf{g}^T = [g_{00}, g_{10}, g_{01}, g_{20}, \dots, g_{0n}]. \tag{2.11}$$

By solving $\mathbf{b}(\mathbf{x}) = \mathbf{M}^{-1}(\mathbf{x}) \mathbf{g}(\mathbf{x})$ from Eq. (2.9), the regularized weight function $\tilde{w}_a(\mathbf{x}; \mathbf{x} - \mathbf{s})$ in RKSR is obtained by

$$\tilde{w}_a(\mathbf{x}; \mathbf{x} - \mathbf{s}) = \mathbf{g}^T \mathbf{M}^{-1}(\mathbf{x}) \mathbf{H}(\mathbf{x} - \mathbf{s}) w_a(\mathbf{x} - \mathbf{s}). \tag{2.12}$$

Since the regularized weight function \tilde{w}_a is constructed to meet the gradient reproducing conditions in Eq. (2.5), we have the following relation between RKSR and gradient model:

$$\begin{aligned}
 \tilde{\varepsilon}(\mathbf{x}) &= \int_{\Omega} \tilde{w}_a(\mathbf{x}; \mathbf{x} - \mathbf{s}) \varepsilon(\mathbf{s}) \, d\mathbf{s} \\
 &= \mathbf{g}^T(\mathbf{x}) \mathbf{M}^{-1}(\mathbf{x}) \int_{\Omega} \mathbf{H}^T(\mathbf{x} - \mathbf{s}) \varepsilon(\mathbf{s}) w_a(\mathbf{x} - \mathbf{s}) \, d\mathbf{s} \quad (\text{continuous RKSR}) \\
 &= \varepsilon(\mathbf{x}) + \sum_{i+j=1}^n \alpha_{ij} D_{ij} \varepsilon(\mathbf{x}) + R \quad (\text{gradient reproduction}).
 \end{aligned} \tag{2.13}$$

Since the gradient reproducing conditions are only imposed up to n th order monomials, the difference between the n th order RKSR in Eq. (2.13) and the n th order gradient model in Eq. (2.4) is of order $n + 1$,

Table 1
Reproduction of strain and its derivatives

\mathbf{g}^T	Order of basis functions n	$\tilde{\varepsilon}(\mathbf{x}) = \mathbf{g}^T \mathbf{M}^{-1}(\mathbf{x}) \int_{\Omega} \mathbf{H}^T(\mathbf{x} - \mathbf{s}) \varepsilon(\mathbf{s}) w_a(\mathbf{x} - \mathbf{s}) \, d\mathbf{s}$ implicit gradient model
[1]	1	$\tilde{\varepsilon}(\mathbf{x}) = \varepsilon(\mathbf{x})$
[1, 0, 2c]	2	$\tilde{\varepsilon}(\mathbf{x}) = \varepsilon(\mathbf{x}) + c \nabla^2 \varepsilon(\mathbf{x})$
[1, 0, 2c ₁ , 24c ₂]	4	$\tilde{\varepsilon}(\mathbf{x}) = \varepsilon(\mathbf{x}) + c_1 \nabla^2 \varepsilon(\mathbf{x}) + c_2 \nabla^4 \varepsilon(\mathbf{x})$

and is represented by a remainder (truncation) R . Table 1 lists the one-dimensional RKSR method with different orders of regularization.

3. Discrete reproducing kernel strain regularization

The discretization of the continuous RKSR introduces errors in the discretization of Eq. (2.13). As a consequence, the gradient reproducing conditions are no longer satisfied and the relation between RKSR and gradient model no longer holds when discretization is introduced. To resolve this problem, we consider herein a discrete form of the regularization equation, and introduce *discrete gradient reproducing conditions* so that the gradient terms are reproduced exactly in the discrete form. The procedure is described below; it is a generalization of the procedure for gradient correction given in Krongauz and Belytschko [17].

Let us first write the discrete counterpart of the continuous regularization equation (2.2) at the following sum:

$$\tilde{\varepsilon}(\mathbf{x}) = \sum_{I=1}^{NP} \tilde{w}_a(\mathbf{x}; \mathbf{x} - \mathbf{x}_I) \varepsilon(\mathbf{x}_I), \tag{3.1}$$

where NP is the number of discrete points, \mathbf{x}_I is the position vector of point I , and \tilde{w}_a is the regularized weight function centered at \mathbf{x}_I :

$$\tilde{w}_a(\mathbf{x}; \mathbf{x} - \mathbf{x}_I) = \left(\sum_{i+j=0}^n (x_1 - x_{1I})^i (x_2 - x_{2I})^j b_{ij}(\mathbf{x}) \right) w_a(\mathbf{x} - \mathbf{x}_I) \equiv \mathbf{H}^T(\mathbf{x} - \mathbf{x}_I) \mathbf{b}(\mathbf{x}) w_a(\mathbf{x} - \mathbf{x}_I). \tag{3.2}$$

The vector $\mathbf{b}(\mathbf{x})$ is obtained by imposing the following *discrete gradient reproducing conditions*:

$$\sum_{I=1}^{NP} x_{1I}^p x_{2I}^q \tilde{w}_a(\mathbf{x}; \mathbf{x} - \mathbf{x}_I) = x_1^p x_2^q + \sum_{i+j=0}^n \alpha_{ij} D_{ij}(x_1^p x_2^q), \quad 0 \leq p + q \leq n, \quad \alpha_{00} = 0. \tag{3.3}$$

It can be shown that the above equation is equivalent to

$$\sum_{I=1}^{NP} (x_1 - x_{1I})^p (x_2 - x_{2I})^q \tilde{w}_a(\mathbf{x}; \mathbf{x} - \mathbf{x}_I) = \delta_{p0} \delta_{q0} + \alpha_{pq} (-1)^{p+q} p! q!, \quad 0 \leq p + q \leq n, \quad \alpha_{00} = 0. \tag{3.4}$$

Substituting Eq. (3.2) into Eq. (3.4), and expressing Eq. (3.4) explicitly for all $0 \leq p + q \leq n$ we have

$$\begin{aligned} \sum_{I=1}^{NP} \mathbf{H}^T(\mathbf{x} - \mathbf{x}_I) w_a(\mathbf{x} - \mathbf{x}_I) \mathbf{b}(\mathbf{x}) &= 1 = g_{00}, \\ \sum_{I=1}^{NP} (x_1 - x_{1I}) \mathbf{H}^T(\mathbf{x} - \mathbf{x}_I) w_a(\mathbf{x} - \mathbf{x}_I) \mathbf{b}(\mathbf{x}) &= -\alpha_{10} = g_{10}, \\ \sum_{I=1}^{NP} (x_2 - x_{2I}) \mathbf{H}^T(\mathbf{x} - \mathbf{x}_I) w_a(\mathbf{x} - \mathbf{x}_I) \mathbf{b}(\mathbf{x}) &= -\alpha_{01} = g_{01}, \\ \sum_{I=1}^{NP} (x_1 - x_{1I})^2 \mathbf{H}^T(\mathbf{x} - \mathbf{x}_I) w_a(\mathbf{x} - \mathbf{x}_I) \mathbf{b}(\mathbf{x}) &= 2\alpha_{20} = g_{20}, \\ &\vdots \\ \sum_{I=1}^{NP} (x_2 - x_{2I})^n \mathbf{H}^T(\mathbf{x} - \mathbf{x}_I) w_a(\mathbf{x} - \mathbf{x}_I) \mathbf{b}(\mathbf{x}) &= \alpha_{0n} (-1)^n n! = g_{0n}. \end{aligned} \tag{3.5}$$

This leads to a system of discrete equations for $\mathbf{b}(\mathbf{x})$

$$\mathbf{M}(\mathbf{x})\mathbf{b}(\mathbf{x}) = \mathbf{g}, \tag{3.6}$$

where

$$\mathbf{M}(\mathbf{x}) = \sum_{I=1}^{NP} \mathbf{H}(\mathbf{x} - \mathbf{x}_I) \mathbf{H}^T(\mathbf{x} - \mathbf{x}_I) w_a(\mathbf{x} - \mathbf{x}_I). \tag{3.7}$$

Substituting $\mathbf{b}(\mathbf{x}) = \mathbf{M}(\mathbf{x})^{-1} \mathbf{g}$ into Eq. (3.2) leads to a regularized weight function that has the same form as Eq. (2.12), except that the moment matrix $\mathbf{M}(\mathbf{x})$ is expressed as a sum in Eq. (3.7). Since the above derivations are based on the satisfying the gradient reproducing conditions in Eq. (3.3), the reproduction of strain gradient through the discrete RKSR can be obtained:

$$\begin{aligned} \tilde{\varepsilon}(\mathbf{x}) &= \sum_{I=1}^{NP} \tilde{w}_a(\mathbf{x}; \mathbf{x} - \mathbf{x}_I) \varepsilon(\mathbf{x}_I) \\ &= \sum_{I=1}^{NP} \mathbf{g}^T(\mathbf{x}) \mathbf{M}^{-1}(\mathbf{x}) \mathbf{H}^T(\mathbf{x} - \mathbf{x}_I) w_a(\mathbf{x} - \mathbf{x}_I) \varepsilon(\mathbf{x}_I) \quad (\text{discrete RKSR}) \\ &= \varepsilon(\mathbf{x}) + \sum_{i+j=1}^n \alpha_{ij} D_{ij} \varepsilon(\mathbf{x}) + R \quad (\text{gradient reproduction}). \end{aligned} \tag{3.8}$$

Here R represents the remainder (truncation). Similar to the continuous case, the difference between n th order discrete RKSR in Eq. (3.8) and the n th gradient model in Eq. (2.4) is of order $n + 1$.

In the discrete RKSR, the regularized weight function $\tilde{w}_a(\mathbf{x}; \mathbf{x} - \mathbf{x}_I)$ is obtained by satisfying reproducing conditions of Eq. (3.3) at any location \mathbf{x} in the domain and boundaries. Thus the resulting discrete RKSR can reproduce strain and its derivatives everywhere in the problem domain and boundaries. This is true regardless that fact that the support of the weight function $w_a(\mathbf{x} - \mathbf{x}_I)$ near the boundary is partially outside the problem domain; the correction function $(x_1 - x_{1I})^i (x_2 - x_{2I})^j b_{ij}(\mathbf{x})$ in Eq. (3.2) corrects the boundary effect. In the following example, we show for a given function $P(x)$, how discrete RKSR $\sum_{I=1}^{NP} \tilde{w}_a(x; x - x_I) P(x_I)$ reproduces $P(x) + \alpha P(x)_{,xx} + \beta P(x)_{,xxxx}$. Two cases are considered (a) $P(x) = x^4$, $0 \leq x \leq 1$, and (b) $P(x) = x \sin(x)$, $0 \leq x \leq \pi$, and $\alpha = \beta = 0.1$. In RKSR, fourth order basis functions and a cubic B-spline weight function w_a are used, and $\mathbf{g}^T = [1, 0, 2\alpha, 0, 24\beta]$. The domain is discretized by 41

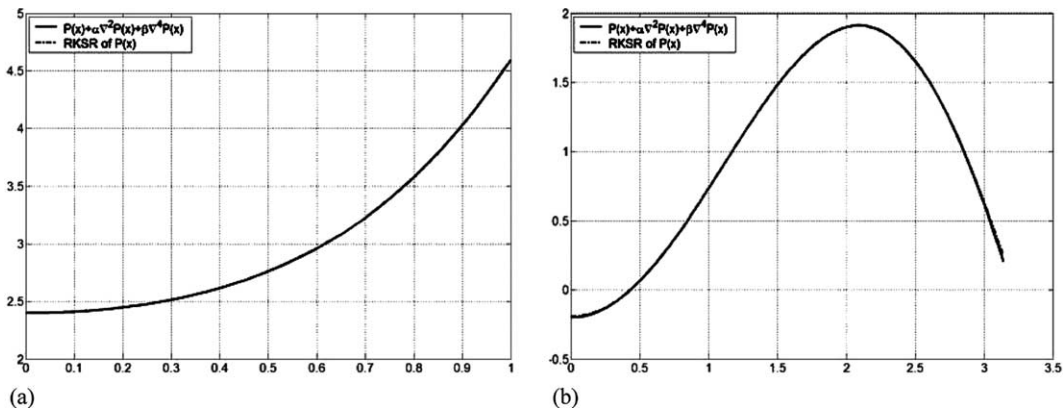


Fig. 1. Reproduction of $P(x) + \alpha P(x)_{,xx} + \beta P(x)_{,xxxx}$ using RKSR $\sum_{I=1}^{NP} \tilde{w}_a(x; x - x_I) P(x_I)$: (a) $P(x) = x^4$, $0 \leq x \leq 1$, and (b) $P(x) = x \sin(x)$, $0 \leq x \leq \pi$.

points, and the support of w_a is chosen to be 4.5 times the nodal distance for the moment matrix $\mathbf{M}(x)$ to be invertible. The results for cases (a) and (b) are shown in Fig. 1(a) and (b), respectively. For case (a), since P is a fourth order polynomial, RKSR exactly reproduces $P(x) + \alpha P(x)_{,xx} + \beta P(x)_{,xxxx}$. For case (b), although not exact, the error is negligible everywhere in the domain as well as on the boundaries.

4. Solution procedures

4.1. Weak form and Galerkin approximation

In the discretization of the equilibrium equation with the RKSR regularized strain, it is crucial that an assumed strain weak form be used [26,27]. In this approach equilibrium corresponds to

$$\delta \Pi(\mathbf{u}, \tilde{\boldsymbol{\varepsilon}}) = \int_{\Omega} \delta \tilde{\boldsymbol{\varepsilon}}^T \boldsymbol{\tau}(\tilde{\boldsymbol{\varepsilon}}) d\Omega - \int_{\Omega} \delta \mathbf{u}^T \mathbf{b} d\Omega - \int_{\Gamma^h} \delta \mathbf{u}^T \mathbf{h} d\Gamma = 0 \quad \forall \mathbf{u} \in H_g^0, \tilde{\boldsymbol{\varepsilon}} \in L_2, \tag{4.1}$$

where $\tilde{\boldsymbol{\varepsilon}}^T = [\tilde{\varepsilon}_{11}, \tilde{\varepsilon}_{22}, 2\tilde{\varepsilon}_{12}]$ is the regularized strain, $\boldsymbol{\tau}^T = [\tau_{11}, \tau_{22}, \tau_{12}]$ is the stress computed from the regularized strain, $\mathbf{u}^T = [u_1, u_2]$ is the displacement vector, \mathbf{b} is the body force vector, \mathbf{h} is the surface traction vector, Ω is the problem domain, and Γ^h is the traction boundary.

Let the displacement approximation be expressed in the following form:

$$u_i^h(\mathbf{x}) = \sum_{I=1}^{NP} \Psi_I(\mathbf{x}) d_{iI}, \tag{4.2}$$

where $\Psi_I(\mathbf{x})$ is the displacement shape function, and d_{iI} is the coefficient of the i th component of the approximation. The approximation of the regularized strain $\tilde{\boldsymbol{\varepsilon}}$ is obtained by substituting u_i^h into the discrete strain regularization equation (3.8):

$$\begin{aligned} \tilde{\varepsilon}_{ij}^h(\mathbf{x}) &= \sum_{J=1}^{NP} \tilde{w}_a(\mathbf{x}; \mathbf{x} - \mathbf{x}_J) \varepsilon_{ij}^h(\mathbf{x}_J) \\ &= \frac{1}{2} \sum_{J=1}^{NP} \tilde{w}_a(\mathbf{x}; \mathbf{x} - \mathbf{x}_J) \left(\frac{\partial u_i^h(\mathbf{x}_J)}{\partial x_j} + \frac{\partial u_j^h(\mathbf{x}_J)}{\partial x_i} \right) \\ &= \frac{1}{2} \sum_{J=1}^{NP} \tilde{w}_a(\mathbf{x}; \mathbf{x} - \mathbf{x}_J) \sum_{I=1}^{NP} (\Psi_{I,j}(\mathbf{x}_J) d_{iI} + \Psi_{I,i}(\mathbf{x}_J) d_{jI}) \\ &= \frac{1}{2} \sum_{I=1}^{NP} (\tilde{b}_{iI}(\mathbf{x}) d_{jI} + \tilde{b}_{jI}(\mathbf{x}) d_{iI}) \end{aligned} \tag{4.3}$$

and

$$\tilde{b}_{iI}(\mathbf{x}) = \sum_{J=1}^{NP} \tilde{w}_a(\mathbf{x}; \mathbf{x} - \mathbf{x}_J) \Psi_{I,i}(\mathbf{x}_J), \tag{4.4}$$

where \tilde{w}_a is the regularized weight function in strain regularization of Eq. (3.2). This yields the following approximation of the regularized strain:

$$\tilde{\boldsymbol{\varepsilon}}^h(\mathbf{x}) = \sum_{I=1}^{NP} \tilde{\mathbf{B}}_I(\mathbf{x}) \mathbf{d}_I, \tag{4.5}$$

where

$$\tilde{\mathbf{B}}_I(\mathbf{x}) = \begin{bmatrix} \tilde{b}_{1I}(\mathbf{x}) & 0 \\ 0 & \tilde{b}_{2I}(\mathbf{x}) \\ \tilde{b}_{2I}(\mathbf{x}) & \tilde{b}_{1I}(\mathbf{x}) \end{bmatrix}, \quad \mathbf{d}_I = [d_{1I}, d_{2I}]. \tag{4.6}$$

Introducing approximation functions for \mathbf{u} and $\tilde{\boldsymbol{\varepsilon}}$ in Eqs. (4.2) and (4.5), respectively, into the linearization variational equation (4.1) leads to the following discrete equation:

$$\mathbf{K} \Delta \mathbf{d} = \mathbf{f}^{\text{ext}} - \mathbf{f}^{\text{int}}, \tag{4.7}$$

where

$$\mathbf{K}_{IJ} = \int_{\Omega} \tilde{\mathbf{B}}_I^T \mathbf{C} \tilde{\mathbf{B}}_J d\Omega, \tag{4.8}$$

$$\mathbf{f}_I^{\text{ext}} = \int_{\Omega} \Psi_I \mathbf{b} d\Omega + \int_{\Gamma^h} \Psi_I \mathbf{h} d\Gamma, \tag{4.9}$$

$$\mathbf{f}_I^{\text{int}} = \int_{\Omega} \tilde{\mathbf{B}}_I^T \boldsymbol{\tau}(\tilde{\boldsymbol{\varepsilon}}) d\Omega, \tag{4.10}$$

and \mathbf{C} is the incremental stress–strain constitutive tensor.

4.2. One-dimensional damage induced strain localization

This example demonstrates how reproducing kernel strain regularization regularizes the solution in finite elements in the presence of strain softening. A rod is subjected to a uniaxial tensile deformation by a prescribed displacement as shown in Fig. 2. The strain-based elastic damage law [20] is introduced as follows:

$$\boldsymbol{\tau} = (1 - D)E\boldsymbol{\varepsilon}. \tag{4.11}$$

The corresponding incremental constitutive law is

$$\Delta \boldsymbol{\tau} = (1 - D)E \Delta \boldsymbol{\varepsilon} - E\boldsymbol{\varepsilon} \Delta D, \tag{4.12}$$

$$\Delta D = \begin{cases} 0 & \text{if } \tilde{\varepsilon}_{\text{eq}} < k, \\ \frac{\partial D}{\partial k} \Delta \tilde{\varepsilon}_{\text{eq}} = \frac{\partial D}{\partial k} \tilde{\mathbf{B}} \Delta \mathbf{u} & \text{otherwise,} \end{cases} \tag{4.13}$$

where $0 \leq D \leq 1$ is the scalar damage parameters, and k is the damage threshold. Here, we consider the following damage function:

$$D(\boldsymbol{\varepsilon}) = \begin{cases} \frac{\varepsilon_c(\boldsymbol{\varepsilon} - \boldsymbol{\varepsilon}_i)}{\boldsymbol{\varepsilon}(\boldsymbol{\varepsilon}_c - \boldsymbol{\varepsilon}_i)} & \text{if } \boldsymbol{\varepsilon}_i \leq \boldsymbol{\varepsilon} \leq \boldsymbol{\varepsilon}_c, \\ 1 & \text{if } \boldsymbol{\varepsilon} > \boldsymbol{\varepsilon}_c. \end{cases} \tag{4.14}$$

Eqs. (4.11) and (4.14) represent a linear softening behavior as shown in Fig. 3.

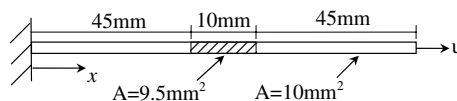


Fig. 2. One-dimensional bar model.

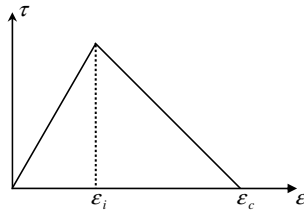


Fig. 3. Linear softening stress–strain relation of 1-D elastic damage model.

Table 2
Parameters in the second order and fourth order RKSR

	Displacement shape function		Strain regularization		RKSR coefficients
	Order of basis function m	Support size	Order of basis function n	Support size	
Second order of regularization	3	3.5	2	2.0	$\mathbf{g}^T = [1, 0, 2c]$ $c = 0.0408$
Fourth order of regularization	5	5.25	4	4.0	$\mathbf{g}^T = [1, 0, 2c_1, 0, 24c_2]$ $c_1 = 0.0408, c_2 = 6.67e-4$

The following parameters are used: $\epsilon_i = 1.0 \times 10^{-4}$, $\epsilon_c = 6.25 \times 10^{-3}$, and $E = 2 \times 10^6$ N/mm². An imperfection of the cross sectional area between $x = 45$ and 55 mm is introduced to initiate bifurcation from a homogeneous state of deformation as shown in Fig. 2. It is expected that the strain will localize in the imperfection zone, while the rest of the structure will relax elastically.

In this problem the following reproducing kernel shape function for displacement is considered:

$$\Psi_I(\mathbf{x}) = \mathbf{H}^T(\mathbf{0})\mathbf{M}(\mathbf{x})^{-1}\mathbf{H}(\mathbf{x} - \mathbf{x}_I)\Phi_a(\mathbf{x} - \mathbf{x}_I), \tag{4.15}$$

where $\mathbf{H}^T(\mathbf{x} - \mathbf{x}_I) = [1, x_1 - x_{1I}, x_2 - x_{2I}, \dots, (x_2 - x_{2I})^m]$ is a vector of complete m th order basis functions, and Φ_a is the kernel function used in the reproducing kernel approximation [10,11,21,22]. For simplicity, we choose $\Phi_a = w_a$, and $m = n + 1$. Table 2 lists RKSR parameters used in this study.

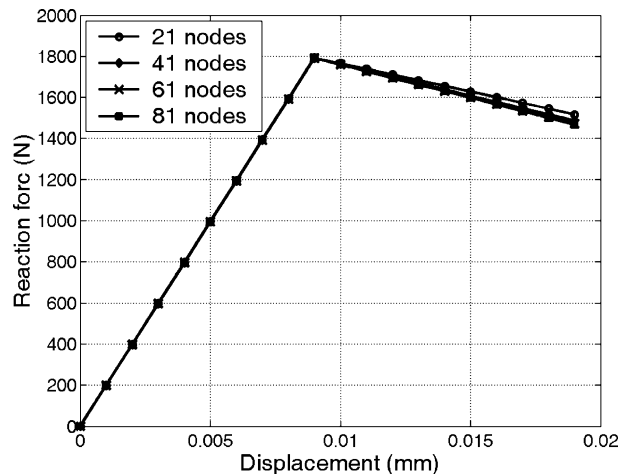


Fig. 4. Force–displacement curves obtained by second order RKSR.

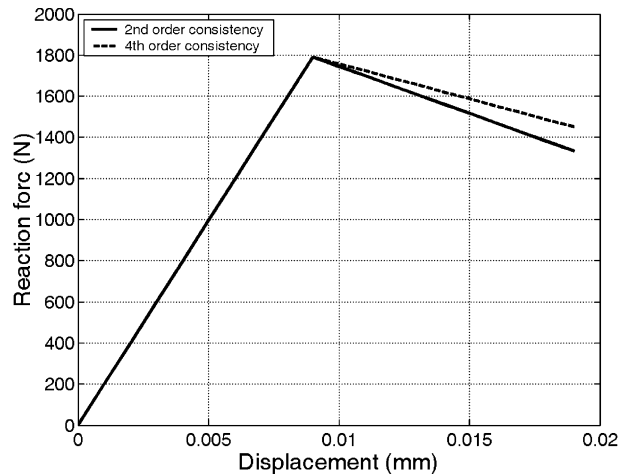


Fig. 5. Force–displacement curves obtained by second and fourth order RKSR.

The force–displacement curves obtained using four spatial discretizations regularized with the second order RKSR shown in Fig. 4 demonstrate a mesh-independent results using of the proposed method. Fig. 5 compares the force–displacement curves obtained using second and fourth order RKSR (corresponding to second and fourth order gradient models), and the fourth order regularized solution shows a slight stiffer response in the softening region. This indicates a stronger regularization effect in the higher order RKSR. Correspondingly, slightly wider strain localization and damage profiles exist in the fourth order RKSR compared to those of the second order RKSR as shown in Figs. 6 and 7, respectively.

As demonstrated in this example, RKSR is capable of introducing gradient type regularization in the strain without the requirement of imposing additional boundary conditions. Moreover, the higher order continuity of the displacements requested in the gradient theory is not needed in the proposed RKSR.

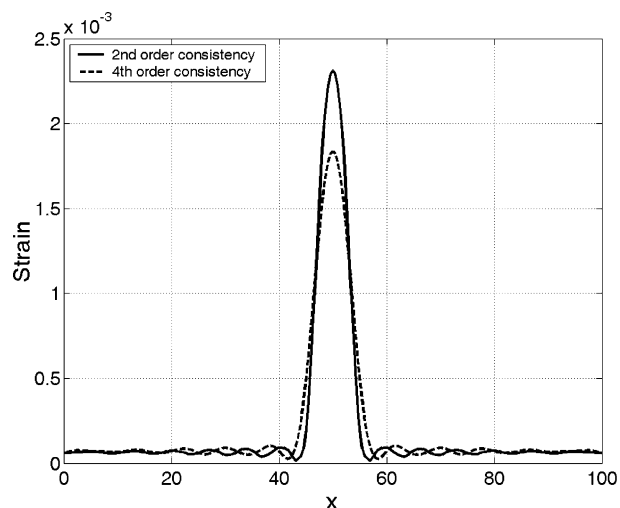


Fig. 6. Strain profiles obtained by second order and fourth order RKSR.

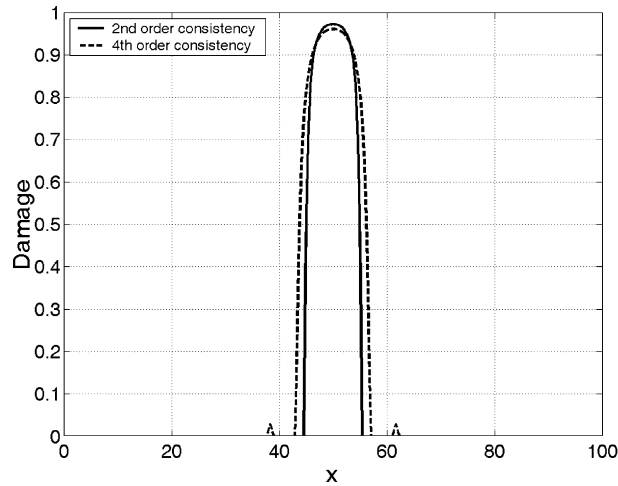


Fig. 7. Damage profiles obtained by second order and fourth order RKSr.

5. von Neumann spectral analysis

5.1. von Neumann formulation

In dynamic problems, classical continuum description with strain softening results in the emergence of an exponential growth of all spectral components and thus it develops a non-physical localized deformation of measure zero. Regularization of the classical continuum stabilizes the short waves and thus yields standing waves with non-zero width. In order to investigate the properties of the regularization methods, a von Neumann analysis on semi-discretization of the following wave equation is carried out:

$$\frac{\partial^2 u}{\partial t^2} = c^2 \left(\frac{\partial^2 u}{\partial x^2} + \frac{\partial^2 u}{\partial y^2} \right), \tag{5.1}$$

where c is the wave speed. The semi-discretization of weak form corresponding to Eq. (5.1) for an infinite domain is

$$\mathbf{M}\ddot{\mathbf{d}} + \mathbf{K}\mathbf{d} = 0, \tag{5.2}$$

where \mathbf{M} and \mathbf{K} are the mass and stiffness matrices, respectively.

$$M_{IJ} = \int_{\Omega} \rho \Psi_I \Psi_J \, d\Omega, \tag{5.3}$$

$$K_{IJ} = \int_{\Omega} c^2 (\tilde{b}_{1I} \tilde{b}_{1J} + \tilde{b}_{2I} \tilde{b}_{2J}) \, d\Omega \tag{5.4}$$

and \tilde{b}_{iI} is the regularized gradient defined in Eq. (4.4). In this paper, the consistent mass matrix in Eq. (5.3) is adopted. To perform the spectral analysis, consider a plane wave in an infinite domain

$$u(x, y, t) = u_0 \exp[ik(x \cos \theta + y \sin \theta) - i\omega t], \tag{5.5}$$

where u_0 is the wave amplitude, k is the wave number, θ is the wave propagation direction, and ω is the circular frequency. The above classical continuum wave equation is non-dispersive, and the phase velocity

(ω/k) is the same as the wave speed c . When regularization is introduced in the classical continuum, the system may become dispersive, and in this case the phase velocity is a function of wave number.

The corresponding discrete form of plane wave solution at point (m, n) with coordinate (x_m, y_n) is:

$$u(x_m, y_n, t) = u_0 \exp[ik(x_m \cos \theta + y_n \sin \theta) - i\bar{\omega}t], \tag{5.6}$$

where $\bar{\omega}$ is numerical circular frequency, and $\bar{c} = \bar{\omega}/k$ is the numerical phase speed. Note that the spatial discretization can introduce numerical dispersion. By considering a uniform space discretization $x_{m+i} = x_m + i \Delta x$; $y_{n+j} = y_n + j \Delta y$, the discrete form of plane wave solution at point $(m + i, n + j)$ with coordinate (x_{m+i}, y_{n+j}) is:

$$u(x_{m+i}, y_{n+j}, t) = u_{m,n} \exp[ik(i \Delta x \cos \theta + j \Delta y \sin \theta) - i\bar{\omega}t], \tag{5.7}$$

where $u_{m,n} = u_0 \exp[ik(x_m \cos \theta + y_n \sin \theta) - i\bar{\omega}t]$. The semi-discretized wave equation (Eq. (5.2)) at particle (x_m, y_n) is:

$$\sum_{i=-I}^I \sum_{j=-J}^J [\mathbf{M}_{(m,n)(m+i,n+j)} \ddot{u}_{m+i,n+j} + \mathbf{K}_{(m,n)(m+i,n+j)} u_{m+i,n+j}] = 0. \tag{5.8}$$

Substituting Eq. (5.7) into Eq. (5.8), we obtain the equation for the circular frequency $\bar{\omega}$:

$$\begin{aligned} & -\bar{\omega}^2 \sum_{i=-I}^I \sum_{j=-J}^J \mathbf{M}_{(m,n)(m+i,n+j)} \exp[ik(i \Delta x \cos \theta + j \Delta y \sin \theta)] \\ & + \sum_{i=-I}^I \sum_{j=-J}^J \mathbf{K}_{(m,n)(m+i,n+j)} \exp[ik(i \Delta x \cos \theta + j \Delta y \sin \theta)] = 0. \end{aligned} \tag{5.9}$$

Introducing the normalized phase velocity $\Theta = \bar{c}/c$, where $\bar{c} = \bar{\omega}/k$ is numerical phase velocity, we have

$$\Theta = \frac{1}{ck} \sqrt{\frac{\sum_{i=-I}^I \sum_{j=-J}^J \mathbf{K}_{(m,n)(m+i,n+j)} \exp[ik(i \Delta x \cos \theta + j \Delta y \sin \theta)]}{\sum_{i=-I}^I \sum_{j=-J}^J \mathbf{M}_{(m,n)(m+i,n+j)} \exp[ik(i \Delta x \cos \theta + j \Delta y \sin \theta)]}}. \tag{5.10}$$

For one-dimension, the normalized phase velocity in Eq. (5.10) can be reduced to

$$\Theta = \frac{1}{ck} \sqrt{\frac{\sum_{i=-I}^I \mathbf{K}_{m,m+i} \cos(ki \Delta x)}{\sum_{i=-I}^I \mathbf{M}_{m,m+i} \cos(ki \Delta x)}}. \tag{5.11}$$

In the following numerical examples, a non-dimensional wave number defined as $k = k \Delta x/\pi$ is used.

5.2. Dispersion analysis

5.2.1. Effects of gradient reproducing conditions

In this example, we study the effects of gradient regularization on the dispersion characteristics in wave propagation. Six cases of RKSR are considered in this study:

- (a) $n = 1, \mathbf{g}^T = [1, 0]$,
- (b) $n = 2, \mathbf{g}^T = [1, 0, 0]$,
- (c) $n = 2, \mathbf{g}^T = [1, 0, 0.05]$,
- (d) $n = 2, \mathbf{g}^T = [1, 0, 0.16]$,
- (e) $n = 4, \mathbf{g}^T = [1, 0, 0.1, 0, 0.015]$,
- (f) $n = 4, \mathbf{g}^T = [1, 0, 0.1, 0, 0.025]$.

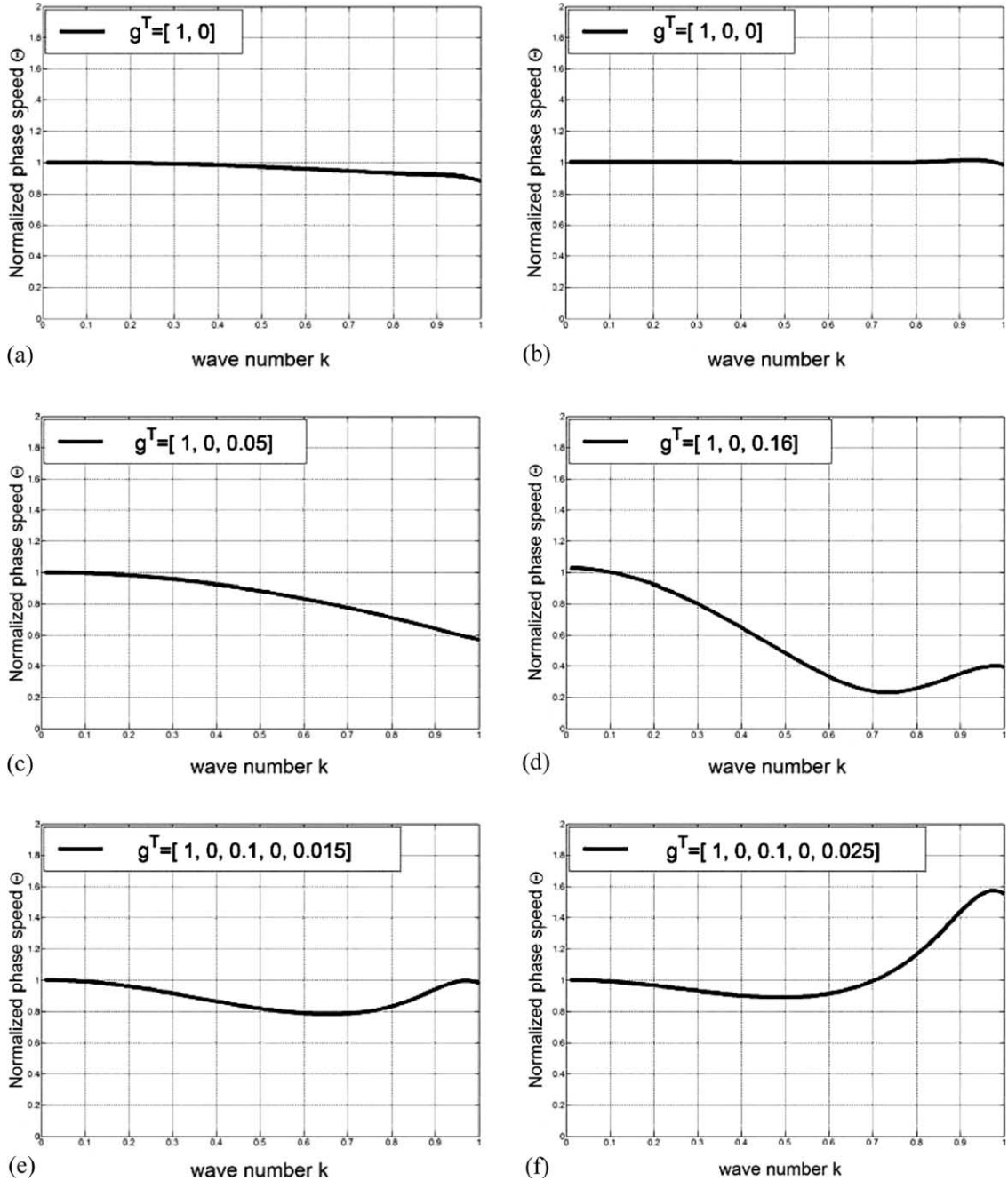


Fig. 8. Normalized phase speed vs. non-dimensional wave number for different gradient reproducing conditions.

We first consider the RKSR cases (a) and (b). In both cases, since no gradient terms are reproduced in the strain regularization as discussed in Section 3, they reduce to the classical continuum with first and second completeness in the strain field. This is reflected in the almost non-dispersive behavior as shown in Fig. 8(a) and (b). Note that the small dispersions are due to the numerical dispersion error in spatial discretization.

In cases (c) and (d), RKSR reproduces strain in the following form

$$\tilde{\varepsilon}(x) = \sum_{I=1}^{NP} \tilde{w}_a(x; x - x_I) \varepsilon(x_I) = \varepsilon(x) + c\varepsilon(x)_{,xx} \tag{5.12}$$

with $c = 0.025$ and 0.08 , respectively, for case (c) and (d). The results in Fig. 8(c) and (d) shows how larger coefficient in the gradient term introduces stronger dispersion to the system. Similarly, the \mathbf{g} vector specified in cases (e) and (f) corresponds to the following reproduction of strain gradient:

$$\tilde{\varepsilon}(x) = \sum_{I=1}^{NP} \tilde{w}_a(x; x - x_I) \varepsilon(x_I) = \varepsilon(x) + c_1\varepsilon(x)_{,xx} + c_2\varepsilon(x)_{,xxxx} \tag{5.13}$$

with $c_1 = 0.1/2!$ and $c_2 = 0.015/4!$ for case (e), and $c_1 = 0.1/2!$ and $c_2 = 0.025/4!$ for case (f). Both cases introduce second and fourth order gradient terms in the strain regularization. It is shown that the introduction of fourth order gradient term with positive coefficients in the strain regularization leads to a normalized phase speed higher than 1 when wave numbers are beyond certain range. This is a non-physical response, similar to the results reported in [1] based on the fourth order gradient model.

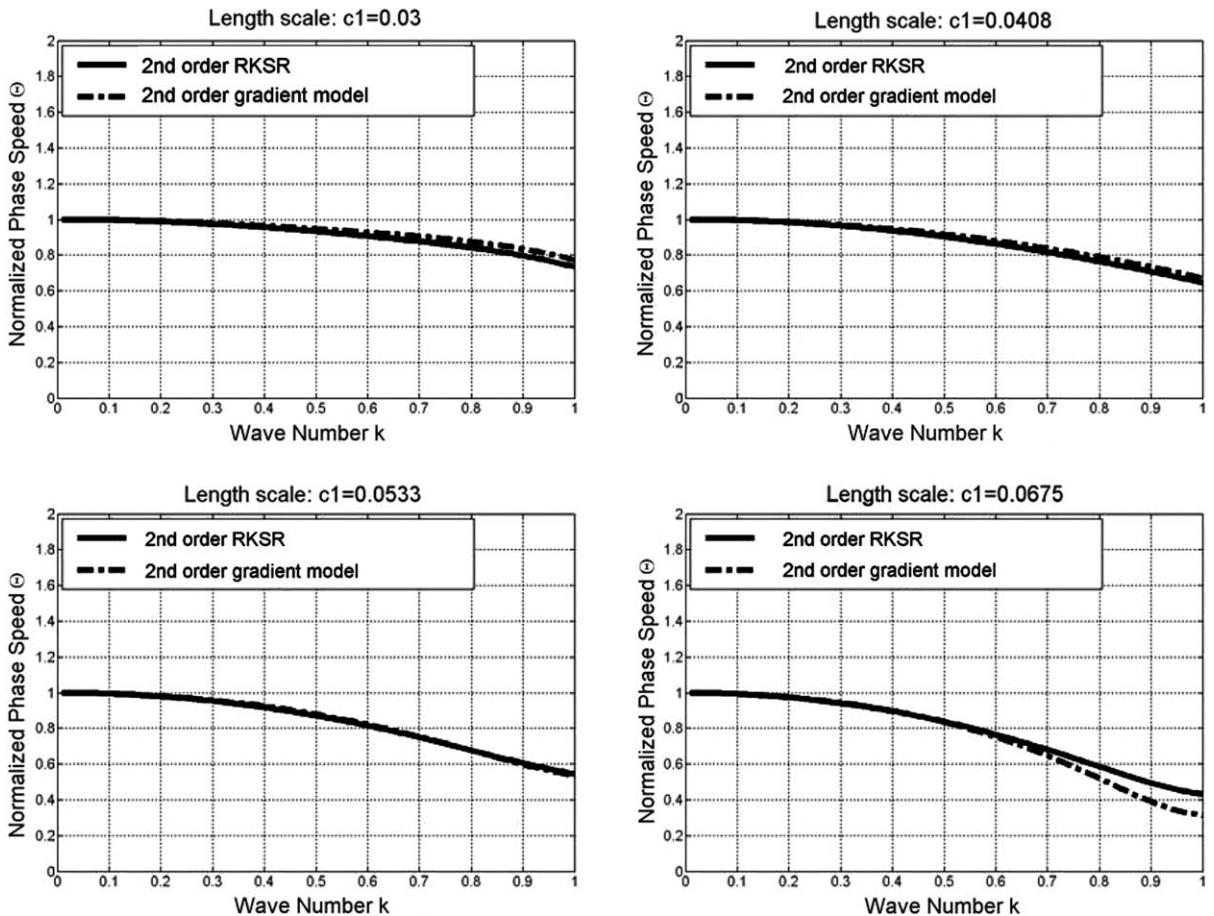


Fig. 9. Normalized phase speeds of the second order regularization methods with positive regularization coefficients.

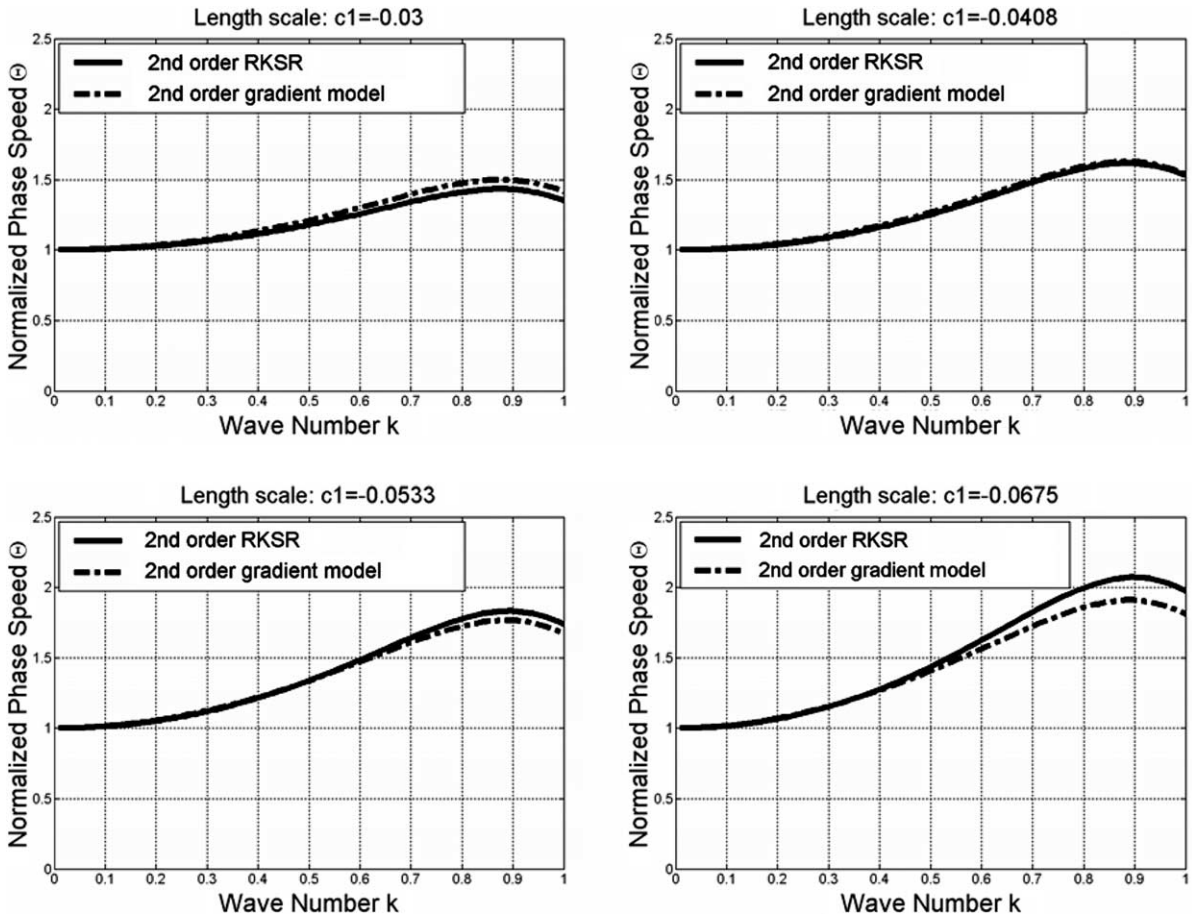


Fig. 10. Normalized phase speeds of the second order regularization methods with negative regularization coefficients.

5.2.2. Comparison of dispersion properties in RKSR and gradient models

In this study, the dispersion properties of the second and fourth order RKSR are compared to those of the second and fourth order gradient models. The regularization coefficients in both methods follow the relations given in Table 1. As shown in Figs. 9 and 10 for the second order regularizations with positive and negative regularization coefficients, respectively, results of RKSR and gradient models are in very good agreement. In these two figures, various values of coefficient of the second order gradient term (c_1) are employed. In the case of the second order regularization with positive regularization coefficients presented in Fig. 9, stronger dispersion is achieved by increasing the coefficient of the second order gradient term. Continuously increasing the gradient coefficient will lead to the occurrence of a cut-off point with zero phase speed. For wave numbers beyond the cut-off point, the phase velocity becomes imaginary and it leads to instabilities. For the case of the second order regularization with negative regularization coefficients as shown in Fig. 10, it can be seen that the phase speed is faster than the wave speed for all the wave numbers which has no physical meanings. Nevertheless, this avoids the possibility of numerical instability compared to the case with positive regularization coefficient.

For the case of fourth order regularization as shown in Fig. 11, the increase of coefficients in the gradient terms leads to a reduced normalized phase speed for wave numbers below certain range. However, for high

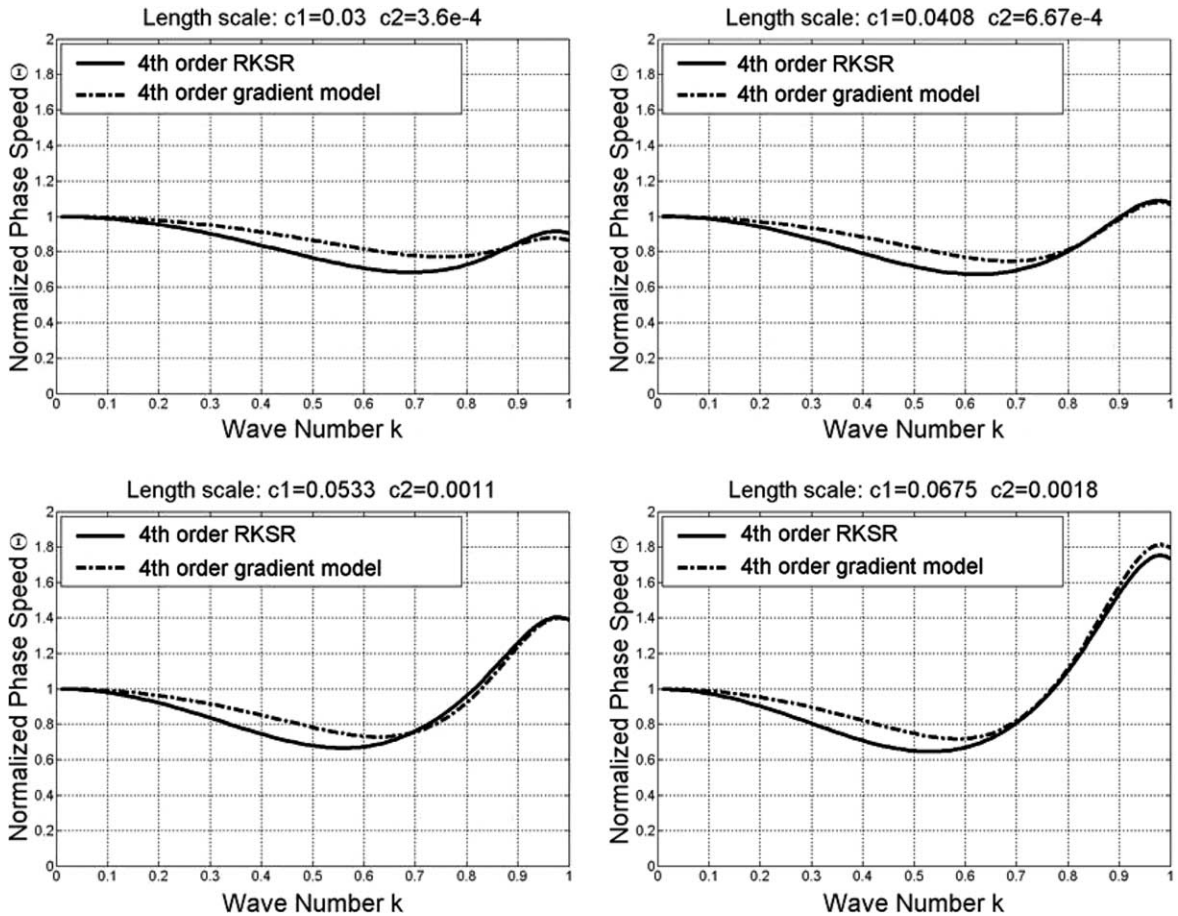


Fig. 11. Normalized phase speeds of the fourth order regularization methods.

wave numbers, the increase of gradient coefficients results in an increase of phase speed, up to a point the normalized phase speed is greater than 1. Thus the fourth order regularization does not yield an instability when large regularization coefficients are employed. On the other hand, this leads to a non-physical situation as the phase speed is faster than the wave speed in the range of large wave numbers as shown in Fig. 11. Similar observation has been reported in [1] using gradient models.

6. Conclusions

An implicit gradient model based on the reproducing kernel strain regularization (RKSR) has been proposed for strain localization problems. We started with a continuous form of RKSR by correcting the weight function in the classical non-local strain representation. The regularized weight function is constructed by imposing gradient reproducing conditions in the regularization equation so that gradients of any order can be reproduced. This approach implicitly introduces gradient type of regularization without increasing the order of governing equation. A major advantage of these methods is that they do not entail any additional boundary conditions, such as commonly found in gradient regularization.

For numerical purposes, a discrete RKSR is also derived. This is *not* based on a direct discretization of continuum RKSR, as this leads to substantial discretization error and hence violation of gradient reproducing conditions. In stead, the discrete RKSR is formulated by imposing the discrete gradient reproducing conditions on a discrete strain regularization equation. This procedure ensures the reproduction of gradients theory in a discrete form. By introducing the displacement shape functions to the discrete RKSR equation, a regularized gradient matrix is obtained and used as the approximation of regularized strain in the weak form of governing equation based on an assumed strain method. Unlike the gradient method which involves formation of several stiffness matrices due to the employment of explicit strain gradient terms [1], the stiffness matrix of the proposed RKSR using assumed strain method takes the standard form, and it only requires replacement of gradient matrix by the regularized gradient matrix.

The ability of the proposed RKSR to resolve mesh sensitivity in damage induced strain localization has been demonstrated. It was also shown that the fourth order regularization model provides a stronger regularization. A von Neumann analysis has been performed to investigate the spectral properties of the RKSR and gradient models. It is shown that RKSR and gradient models yield almost the identical spectral. The numerical results also illustrate that second order regularization could lead to an instability beyond certain wave number range when large regularization coefficients are used. The fourth order regularization, on the other hand, could lead to a non-physical phase speed faster than wave speed for high wave numbers if large regularization coefficients are employed. In this paper, the general form of RKSR for multi-dimensions has been presented. The application of RKSR to two-dimensional strain localization problems will be reported in the forthcoming publication.

Acknowledgement

The support of this work by NSF under grant CMS 0296112 to University of California, Los Angeles is greatly acknowledged.

References

- [1] H. Askes, L.J. Sluys, A classification of higher-order strain gradient models in damage mechanics, *Arch. Appl. Mech.* 72 (2002) 171–188.
- [2] H. Askes, J. Pamin, R. de Borst, Dispersion analysis and element-free Galerkin solutions of second and fourth-order gradient-enhanced damage models, *Int. J. Numer. Methods Engrg.* 49 (6) (2000) 811–832.
- [3] Z.P. Bazant, P.G. Cabot, Nonlocal continuum damage, localization instability and convergence, *ASME, J. Appl. Mech.* 55 (1988) 287–293.
- [4] Z.P. Bazant, T. Belytschko, T.-P. Chang, Continuum model for strain softening, *J. Engrg. Mech.* 110 (1984) 1666–1692.
- [5] Z.P. Bazant, M. Jirasek, Nonlocal integral formulations of plasticity and damage: survey of progress, *J. Engrg. Mech. ASCE* 128 (2002) 1119–1149.
- [6] T. Belytschko, Z.P. Bazant, Y.-W. Hyun, T.-P. Chang, Strain-softening materials and finite-element solutions, *Comput. Struct.* 23 (1986) 163–180.
- [7] T. Belytschko, Y. Krongauz, D. Organ, M. Fleming, P. Krysl, Meshless methods: an overview and recent development, *Comput. Methods Appl. Mech. Engrg.* 139 (1996) 3–49.
- [8] T. Belytschko, Y.Y. Lu, L. Gu, Element-free Galerkin methods, *Int. J. Numer. Methods Engrg.* 37 (1994) 229–256.
- [9] J.S. Chen, C.T. Wu, T. Belytschko, Regularization of material instabilities by meshfree approximations with intrinsic length scales, *Int. J. Numer. Methods Engrg.* 47 (2000) 1301–1322.
- [10] J.S. Chen, H.P. Wang, New boundary condition treatments for meshless computation of contact problems, *Comput. Methods Appl. Mech. Engrg.* 187 (1998) 441–468.
- [11] J.S. Chen, C. Pan, C.T. Wu, W.K. Liu, Reproducing kernel particle methods for large deformation analysis of nonlinear structures, *Comput. Methods Appl. Mech. Engrg.* 139 (1996) 195–227.
- [12] R. de Borst, H.B. Muhlhaus, Gradient-dependent plasticity: formulation and algorithmic aspects, *Int. J. Numer. Methods Engrg.* 35 (1992) 521–539.

- [13] R. de Borst, J. Pamin, Gradient plasticity in numerical simulation of concrete cracking, *Eur. J. Mech., A/Solids* 15 (1996) 295–320.
- [14] R. de Borst, R.H. Pamin, R.H.J. Peerlings, L.J. Sluys, On gradient-enhanced damage and plasticity models for failure in quasi-brittle and frictional materials, *Comput. Mech.* 17 (1996) 130–141.
- [15] J. Feng, K. Wen, X. Tian, Z. Chen, Nonlocal softening model and its application to engineering excavation, *Engrg. Mech. (Chinese Journal)* 16 (6) (1999) 36–43.
- [16] O. Fusao, A. Toshihisa, Y. Atsushi, A strain localization analysis using a viscoplastic softening model for clay, *Int. J. Plast.* 11 (1995) 523–545.
- [17] Y. Krongauz, T. Belytschko, Consistent pseudo-derivatives in the meshless methods, *Comput. Methods Appl. Mech. Engrg.* 146 (1997) 371–386.
- [18] P.V. Lade, Q. Wang, Analysis of shear banding in true triaxial tests on sand, *J. Engrg. Mech.* 127 (8) (2001) 762–768.
- [19] D. Lasry, T. Belytschko, Localization limiters in transient problems, *Int. J. Solids Struct.* 24 (1988) 581–597.
- [20] J. Lemaitre, A continuous damage mechanics model for ductile fracture, *J. Engrg. Mater. Tech.* 107 (1985) 83–89.
- [21] W.K. Liu, S. Jun, S. Li, J. Adee, T. Belytschko, Reproducing kernel particle methods for structural dynamics, *Int. J. Numer. Methods Engrg.* 38 (1995) 1655–1679.
- [22] W.K. Liu, S. Jun, Y. Zhang, Reproducing kernel particle methods, *Int. J. Numer. Methods Fluids* 20 (1995) 1081–1106.
- [23] H.B. Mühlhaus, I. Vardoulakis, The thickness of shear band in granular materials, *Geotechnique* 37 (1987) 271–283.
- [24] A. Needleman, Material rate dependence and mesh sensitivity in localization problems, *Comput. Methods Appl. Engrg.* 67 (1988) 69–85.
- [25] R.H.J. Peerlings, R. de Borst, W.A.M. Brekelmans, J.H.P. de Vree, Gradient enhanced damage for quasi-brittle materials, *Int. J. Numer. Methods Engrg.* 39 (1996) 3391–3403.
- [26] J.C. Simo, T.J.R. Hughes, On the variational foundations of assumed strain methods, *ASME J. Appl. Mech.* 53 (1986) 51–54.
- [27] J.C. Simo, J.W. Ju, Strain- and stress-based continuum damage models—I. Formulation, *Int. J. Solids Struct.* 23 (1987) 821–840.
- [28] L.J. Sluys, Wave propagation, localization and dispersion in softening solids, Ph.D. Thesis, Civil Engineering Department of Delft University of Technology, 1992.